Conf-781022--27

MASTER

STRUCTURAL AND CONTAINMENT RESPONSE TO LMFBR ACCIDENTS

by

J. F. Marchaterre, S. H. Fistedis, L. Baker, Jr.,
D. D. Stepnewski, R. D. Peak, and E. L. Gluekler

Prepared for

International Meeting on
Nuclear Power Reactor Safety

Brussels, Belgium

October 16, 1978

UofC-AUA-USDOE

ARGONNE NATIONAL LABORATORY, ARGONNE, ILLINOIS

Operated under Contract W-31-109-Eng-38 for the
U. S. DEPARTMENT OF ENERGY

STRUCTURAL AND CONTAINMENT RESPONSE TO LMFBR ACCIDENTS

J. F. Marchaterre, S. H. Fistedis, and L. Baker, Jr.
Argonne National Laboratory
Argonne, Illinois 60439

D. D. Stepnewski and R. D. Peak
Hanford Engineering Development Laboratory
Richland, Washington 99352

E. L. Gluekler
General Electric Company
Sunnyvale, California 94086

INTRODUCTION

The adequacy of the containment of fast reactors has been traditionally evaluated by analyzing the response of the containment to a spectrum of core disruptive accidents. The current approach in the U. S. is to consider fast reactor response to accidents in terms of four lines of assurance (LOAs). Thus, LOA-1 is to prevent accidents, LOA-2 is to limit core damage, LOA-3 is to control accident progression and LOA-4 is to attenuate radiological consequences. Thus, the programs on the adequacy of containment response fall into LOA-3.

Significant programs to evaluate the response of the containment to core disruptive accidents and, thereby, to assure control of accident progression are in progress. These include evaluating the mechanical response of the primary system to core disruptive accidents and evaluating the thermal response of the reactor structures to core melting, including the effects this causes on the secondary containment.

The analysis of structural response employs calculated pressure-volume-time loading functions. The results of the analyses establish the response of the containment to the prescribed loadings. The analysis of thermal response requires an assessment of the distribution and state of the fuel, fission products and activated materials from accident initiation to final disposition in a stable configuration.

STRUCTURAL RESPONSE

Significant progress has been made in the evaluation of the response of components and systems to hypothetical core disruptive accidents (HCDA) since

the formalization of this sector of LMFBR technology.[1]

Propagation of HCDA effects through the symmetrical components of the primary system, the elastic-plastic deformation of these components, and the ultimate dissipation of the accident can be treated by REXCO-type Lagrangian, or ICECO-type Eulerian codes. Similar primary system response codes at different levels of sophistication are currently available in several countries.

Although these codes take a systems approach, the main LMFBR components treated by them are the core barrel and the reactor vessel. The deformation and ultimate adequacy of the reactor vessel in sustaining the HCDA effects is important. It constitutes the first barrier to sodium (Na) spillage.

For loop-type LMFBRs, with small reactor vessels, and with mostly concentric components, the 2-dimensional (2D) hydrodynamic-elastic-plastic codes, such as REXCO-HEP[2], ICECO[3], ASTARTE[4], SURBOUM[5], ARES[6], can gauge the HCDA effects reasonably well. The perforated core support structure, and the reactor head cover need special consideration. The core support structure basically requires a 3-dimensional (3D) analysis to determine its adequacy. But for HCDA calculations, treating the vessel internals as a system, 2D approximations are employed. For the reactor cover 3D elastic-plastic codes - such as the ANL-developed SADCAT[7] finite element code - have to be applied. Fig. 1 depicts the finite element grid of a loop-type reactor cover comprised of three eccentric plugs. Codes such as REXCO or ICECO provide the pressure-time history of the sodium slug on the reactor cover, and SADCAT calculates the transient elastic-plastic strains and final deformations of the cover. Fig. 2 shows the finite element grid of the cover for a pool-type reactor. Due to symmetry, only a 12° sector of the cover is shown. Current capability of SADCAT, includes the resistance to deformation of the concrete and its reinforcement in the cover in addition to the webs and flanges shown. The importance of cover response to secondary containment will be taken up later.

For loop-type LMFBRs employ an extensive piping system. If the postulated accident does not require continuous heat removal, then piping problems are reduced. If, on the other hand, heat removal is postulated, the piping system will have to be evaluated for pulses originating in the core region. The ANL-developed ICEPEL[8] code has 2D hydrodynamic-elastic-plastic capability to treat pulses in piping systems. Recently this capability was extended to model reasonably well all other primary system in-line components, except pumps. ICEPEL improvement is currently in progress. Fig. 3 shows a mathematical model of 1/10

intermediate heat exchanger within a simplified heat transport system.

For large pool-type LMFBRs, HCDA treatment and component response cannot be gauged as satisfactorily with 2D codes as in loop-type LMFBRs. Most of the large and important components inside the primary tank are eccentrically located. 2D codes will provide the initial pressure fields in the vicinity of eccentric components, but cannot be relied upon to provide component response. 3D fluid-structure interaction codes are needed. Currently such a code is under development at ANL. Fig. 4 shows a 12° sector of primary tank with the finite element mesh depicting the fluid and the in-tank component.

In an attempt to increase the margin of safety of the large LMFBRs of the future against HCDA and concurrently reduce costs, an adaptation of the PCRV to LMFBR containment is in progress. Prior work on the hydrodynamics of the HCDA is combined with finite element treatment of reinforced concrete possessing prestressing capability in a new ANL code, DYNAPCON. Eventually the endochronic theory of concrete will be incorporated for improved modeling. Concurrent development work is in progress to enable concrete to satisfy unique conditions of LMFBR vessel requirements such as reduction of heat gradients through continuous drying.[9] Fig. 5 shows a conceptual design of a PCRV for a pool-type LMFBR. Similar conceptual designs of PCRV serving a loop-type LMFBR are available. It appears that the PCRV head cover of the loop-type version will have less severe thermal and slug impact problems that the pool-type version.

Calculations show - as expected - that the slug impact is the most serious effect, causing the first cracking of the PCRV at the junction of the vertical wall and the head cover. Fig. 6 shows the cracking sequence at the times indicated for the pool-type PCRV of Fig. 5.

A recent area of concentration pertains to the evaluation of missile and sodium spillage effects on secondary containment. Parametric studies indicate that for the HCDAs considered and possibly for HCDAs one order of magnitude above those currently considered, missiles are not likely to compromise secondary containment. Sodium fires may constitute a more serious problem. In an HCDA, sodium spillage can occur after slug impact through cracks and openings in the head cover. Important assumptions will have to be made as to the size and mode of these openings. SADCAT-type analysis providing the final deformations of the head cover could be helpful in establishing crack sizes and potential sodium paths. Then ICECO, which possesses spillage capability, may be employed to give a rate of sodium ejection into the secondary containment. This will constitute the

input for calculations on sodium fires and resulting pressures in the secondary containment. Fig. 7 shows an ICECO output of an HCDA at three instants, including (a) vessel deformation; first due to the early burst and then due to slug impact; (b) lifting of the reactor cover and stretching of the hold-down bolts; and (c) sodium spillage through the cover and over the side of the vessel.

THERMAL RESPONSE

For some reactor designs, core debris retention may be accomplished within the reactor vessel. However, it is generally found that for large loop-type reactors with small vessels, large core debris masses will penetrate relatively rapidly through the vessel wall, and drain into the reactor cell. The resulting thermal and chemical reactions between core debris, sodium and concrete structures could potentially lead to severe containment loading conditions and radionuclide penetration into the soil or leakage into the air.

In general, it is necessary to demonstrate accommodation of radioactive solids and liquids in the reactor cell with self-limiting debris penetration into the concrete and limited structural damage to the containment walls, or alternatively, demonstrate material retention in the reactor vessel, and to demonstrate adequate retention of radionuclide aerosols, vapors and gases in the containment or controlled release with acceptable consequences.

In a postulated core meltdown accident, the core debris is assumed to be expelled from the original core location in upward and downward directions. Upon contact with subcooled sodium, the core debris is rapidly quenched and fragments into small particles. A series of experiments were performed to determine fragmentation characteristics including completeness of fragmentation, particle size distribution and pressure pulses associated with the interaction. The "M-Series" of experiments was carried out using quantities of thermite-generated core debris of the order of a kilogram. The early experiments, M1, M2, and M3, were performed under "in-vessel conditions" where the molten material was injected into a pool of sodium.[10] The tests demonstrated the marked tendency of core debris to fragment completely in the presence of an excess of sodium. Recent experiments, M5, M6, and M7, were performed under "ex-vessel conditions" where the core debris entered a dry steel-lined cavity and was followed immediately by a flow of sodium at 425°C.[11] The core debris was found to have fragmented completely. Results of particle size distribution measurements are compared in Fig. 8 with results from an experiment involving forced injection

of molten core debris into sodium (EDT-1) and the range of distribution from in-pile tests in TREAT (E2 and S3). Interactions in all cases were incoherent, non-energetic fragmentations and particle dispersions.

The core-debris particulate generated by interaction with sodium tends to settle on available horizontal surfaces forming particulate beds. It has been shown that such beds of internally-heated particles are stable and coolable to a characteristic critical depth beyond which coolant dryout would occur.[12] The maximum temperature for a coolable configuration is necessarily the boiling point of sodium. In a small reactor, such as FFTF, sufficient surface is available so that permanent in-vessel retention of core debris was considered likely.[13] For larger loop-type LMFBR designs, it can be assumed that the primary coolant boundary has sufficient strength at the boiling point of sodium to provide at least temporary core debris retention. Eventually, sodium dryout will cause a significant reduction in heat removal from the bed so that heat up and remelting could result.

During the heat up process, three states with different heat transfer modes could exist: (a) solid fuel and steel particles (b) molten steel with entrained solid fuel particles and (c) molten steel and fuel. To determine the potential for core debris retention, a two-dimensional thermal model of the reactor vessel and adjacent heat absorbing structures was developed.[14] Fig. 9 shows a typical temperature response of the reactor vessel and guard vessel. Complete melt-through of the vessel wall would occur approximately 70 minutes after particle bed dryout. However, structural evaluations using a membrane creep rupture model indicated failure at 20 minutes with significant creep deformation (sagging) preceeding the rupture. The core debris at the time of vessel failure was determined to consist of solid fuel particles entrained in molten steel.

Following vessel failure, the core debris would be expected to form a particulate bed under sodium in the reactor cavity, as noted previously. The reactor cavity, in current designs, is completely lined with steel plate which prevents direct contact between the sodium and the underlying concrete. However, concrete overheating and cracking can occur because of heat transfer from the sodium pool. Surface-heated concrete structures can potentially fail by two failure modes (1) spallation (crack formation parallel to the heated surface under tensile stresses) and (2) crushing because of compressive failure.

To describe the local fracture characteristics of a surface heated concrete structure at elevated temperatures, a failure surface model was developed.[15]

The failure surface was defined in terms of the uniaxial compressive strength of a cylinder, the uniaxial tensile strength, and the biaxial compressive strength. In the model, the surface was approximated by a generalized cone with a parabolic contour centered along the average axis of all principal streses. Failure is encountered when the stress vector resulting from the combined thermal, pore and shear stresses, penetrates through the failure surface. The evaluation of thermal stresses followed standard procedures. Pore stresses were determined from a model in which the open pore structure was divided into three principal coordinate components. The pore pressure was obtained from the COWAR-2 code.[16] This code determines heat and mass transfer in concrete taking into account the evaporation of water, diffusion, filtration and recondensation of water vapor. Maximum pore pressures occur at an evaporation front which slowly advances into the concrete as surface heating is maintained. Figure 10 shows a typical pressure distribution at a depth of 2.5 cm below the surface.

A preliminary investigation of the failure criterion showed that concrete spallation would occur only under extreme conditions such as very high surface temperatures combined with a high free water content and small porosity. This is in agreement with experimental observations. Spallation cracks were observed at a depth of 1.5 to 2.5 cm. This is consistent with predictions by the COWAR-2 Code which indicates a peak pore pressure at these depths.

Local failures of the cavity liner would lead to interaction between sodium and concrete which depends to some extent on the concrete composition. Experiments on the interaction of sodium with the basalt concrete used in the construction of FFTF have been in progress since 1974.[17,18] Recent results are shown in Fig. 11. The tests were performed with concrete cast into 34 cm I. D. pipe and employed sodium temperatures of 510°C to 870°C. The results indicated that the reaction rate decreases with time and is self-limiting because of the accumulation of reaction products. For application to the illustrative containment calculation given in this paper, the data were correlated as follows:

$$x = 7.6(1 - \exp - t/3) \qquad (1)$$

where x is the penetration distance in cm and t is time in hours.

Water vapor, released from the heated concrete, reacts with sodium to form hydrogen which is transported along with sodium vapor and aerosol into the secondary containment. Hydrogen diffuses and mixes rapidly, stratifies only under extremely stagnant conditions, ignites easily and has burning lower limits of 4-9% hydrogen and detonation lower limits of 19-20% hydrogen (in STP

air).[19] A series of experiments have shown that jets of hydrogen and sodium vapor-aerosol will self-ignite in air.[20] In atmospheres having 19-21% oxygen, the sodium concentrations and jet temperatures corresponding to ignition limits are as shown in Fig. 112. Above 790°C, the hydrogen reacts with air even without sodium. The hydrogen and sodium reactions consume the oxygen of the secondary containment and lead to extinguishment of the hydrogen reaction even though the sodium reaction continues. Additional experiments have shown that continuous and complete burning will occur until the secondary oxygen concentration decreases to a range of 5-14%.

A comprehensive computer program CACECO has been developed to predict the thermodynamic responses of primary and secondary containment to a variety of LMFBR facility accidents, such as: (a) loss of space cooling in a pipe-way or cell, (b) sodium leakage as a spray or spill, and (c) HCDA releases.[21] The severity of HCDA responses increases as reactor size increases. A 2500 MWt reactor with containment typical of loop-type LMFBRs was chosen for this example of CACECO usage. The containment model has been described elsewhere.[21] The model includes the reactor cavity, heat transport system (HTS) cells, equipment rooms and the reactor containment building (RCB). The cavity floor is assumed to be a failed steel liner covering 1.83 m of basalt concrete. The HCDA is assumed to lead to a melt-through and a sodium spill of 9.07×10^5 kg of sodium and the sodium reacts with the basalt concrete floor according to Eq. 1. The asymptotic penetration of this reaction, 7.6 cm, is treated in Fig. 13 by the assumption that the reaction product layer has high thermal conductivity. The floor temperature profiles show the gradual heating of concrete; at temperatures above 150°C, 56% of the concrete water is released into the sodium pool and at temperatures above 440°C, 86% is released. The decay power of the core debris and the chemical reactions heat the sodium pool to its boiling point (882°C) in seven to eight hours. Sodium boils from the cavity pool, and its vapor flows through vent passages into the HTS cells, where it cools and condenses. By 174 hours, the cavity has boiled dry with 93 percent (844,200 kg) of the sodium boiled from the cavity into the cells, 7 percent (63,000 kg) was consumed by chemical reactions with oxygen, concrete, and water in the cavity.

The steam released from the heated concrete walls which are protected by an intact liner is assumed to vent through the liner vent piping into the equipment rooms, where it condenses and accumulates. The equipment rooms are heated to the water boiling point in seven hours; thereafter, steam flows up

the stairways into the RCB work space where it heats and pressurizes the RCB. The hydrogen and sodium leakage from the reactor cavity and HTS cells enter the RCB space as multiple jet flows which self-ignite and the chemical reactions heat and pressurize the RCB. By fifteen hours the RCB is pressurized to 62 kPa gage and at this pressure a relief system operates to vent gas, as required to limit the pressure to 69 kPa gage.

The RCB conditions are shown in Fig. 14. By twenty-one hours, the leakage of hydrogen (270 kg) and sodium (450 kg) from the cavity and cells had consumed part of the RCB oxygen and the leakage of steam (53,600 kg) from the equipment room had diluted the remaining oxygen to the extinguishment concentration of 11% assumed in the analysis. Thereafter, the hydrogen accumulated in the RCB but the continual dilution by steam from the equipment room kept the hydrogen at a low concentration. The maximum RCB temperature was only 112°C as steam replaced the initial air atmosphere.

The analysis ended with the cavity boiled dry of sodium. The calculations presented here provide the information needed to compute off-site radiological consequences, principally the rate of sodium transport along with fission products to the RCB, and the rate of RCB leakage to the environs. Following sodium boil-dry, the core debris is no longer cooled by sodium evaporation, and melting of the cavity concrete floor is postulated.

A computer program GROWS II is being developed to provide detailed descriptions of the penetration of the core debris into concrete and other materials. Account is taken of radial as well as of downward growth. GROWS II will enable predictions of the final disposition of the bulk of the fuel and non-volatile radioactive materials.

CONCLUSIONS

Recent advances in understanding are helping to clarify the structural and containment response of fast reactors to core disruptive accidents.

In the area of structural response of LMFBRs to core disruptive accidents, a range of codes have been developed and are under development for analyzing this response. Significant improvements have been made in the analysis of the reactor head cover, including the consideration of the effects of missiles and on including the effects of internal structures.

In the area of thermal response, a wide range of experimental results have been obtained and are being used in conjunction with the development of codes to analyze the effects of core debris on the secondary containment.

REFERENCES

[1] S. H. Fistedis, "Containment of Fast Breeder Reactors - Present Status - Remaining Problems" Invited Lecture, Proceedings of the 1st International Conference on Structural Mechanics in Reactor Technology, Paper E 2/1, Berlin, Germany, September 20-24, 1971.

[2] Y. W. Chang, et al., "Analysis of the Primary Containment Response Using a Hydrodynamic-Elastic-Plastic Computer Code," Proceedings of the 2nd International Conference on Structural Mechanics in Reactor Technology, Paper E 2/1, Berlin, Germany, September 10-14, 1973.

[3] C. Y. Wang, et al., "Application of the Implicit Eulerian Method (ICECO) to Fast Reactor Containment," Proceedings of the 3rd International Conference on Structural Mechanics in Reactor Technology, Paper E 3/4, London, United Kingdom, September 1-5, 1975.

[4] M. S. Cowler, "ASTARTE, A 2D Lagrangian Code for Unsteady Compressible Flow, Theoretical Description" AWRE-44-91-37, March 1974.

[5] M. Stiévenart, et al., "Analysis of LMFBR Explosion Model Experiments by means of the SURBOUM-II Code," Proceedings of the 3rd International Conference on Structural Mechanics in Reactor Technology, London, United Kingdom, September 1-5, 1975.

[6] K. Doerbecker, et al., "Analysis of Mechanical HCDA Consequences with ARES for Demonstration of Primary Containment Integrity in SNR-300." Proceedings of the 4th International Conference on Structural Mechanics in Reactor Technology, Paper E 1/5, San Francisco, California, U.S.A., August 15-19, 1977.

[7] R. F. Kulak, and T. B. Belytschko, "An Implicit Three-Dimensional Finite Element Formulation for Nonlinear Structural Response of Reactor Components," ANL-76-85, July 1976.

[8] M. T. A-Moneim, "Coupled Hydrodynamic-Structural Response Analysis of Piping Systems," ANL-77-91, February 1978.

[9] Z. P. Bazant & S. H. Fistedis, "Dried Hot Concrete Vessel for Nuclear Reactors: Proposal of a Design Concept," Nuclear Engineering and Design, Vol. 47, No. 2, pp. 317-324, May 1978.

[10] T. R. Johnson, L. Baker, Jr., and J. R. Pavlik, "Large-Scale Molten Fuel-Sodium Interaction Experiments," Proc. Fast Reactor Safety Meeting, Beverly Hills, Calif., CONF-740401-P2, April 2-4, 1974, p. 883.

[11] J. D. Gabor, E. S. Sowa, J. R. Pavlik, and J. C. Cassulo, "Particulate Formation and Phenomena," Proc. Third Post-Accident Heat Removal "Information Exchange," Argonne, Ill., ANL-78-10, November 2-4, 1977, p. 74.

[12] J. D. Gabor, E. S. Sowa, L. Baker, Jr., and J. C. Cassulo, "Studies and Experiments on Heat Removal from Fuel Debris in Sodium," Proc. Fast Reactor Safety Meeting, Beverly Hills, Calif., CONF-740401-P2, April 2-4, 1974, p. 823.

[13] "Safety Evaluation Report (FFTF)" NUREG-0358, August 1978.

[14] E. L. Gluekler, R. M. Clever, and E. T. Rumble, "Investigation of the Structural Integrity of the Reactor Vessel for a Postulated Core-Meltdown Accident," Trans. 4th Int. Conf. Structural Mechanics in Reactor Technology, San Francisco, Calif., August 15-19, 1977.

[15] E. L. Gluekler and A. Dayan, "Concrete Failure Modes at Elevated Temperatures," Proc. Third Post-Accident Heat Removal "Information Exchange," Argonne, Ill., ANL-78-10, November 2-4, 1977, p. 233.

[16] A. Dayan, "COWAR-2 User's Manual, Thermo-Hydraulic Behavior of Heated Concrete," GE-FBRD, GEFR-00090(L), May 1977.

[17] J. A. Hassberger, R. K. Hilliard, and L. D. Muhlestein, "Sodium-Concrete Reaction Tests," HEDL-TME 74-369, June 1974.

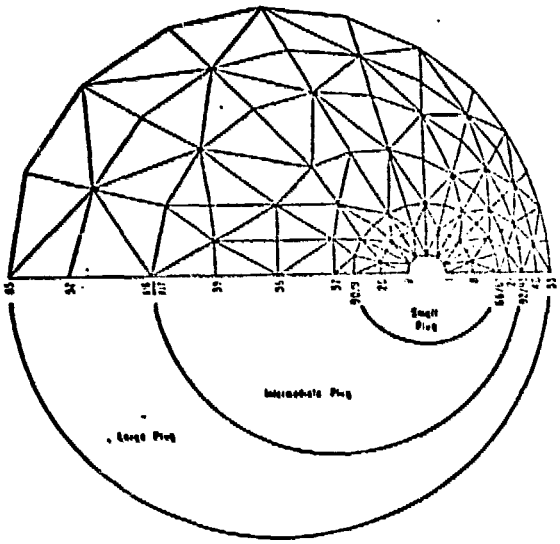

Fig. 1. Finite Element Grid of a Loop-type Reactor Cover

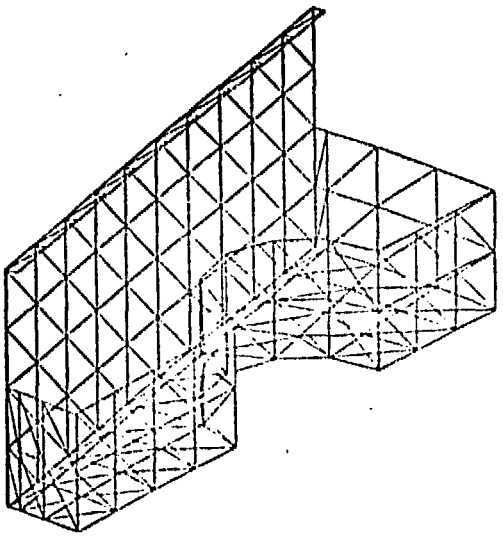

Fig. 2. Finite Element Grid of a Pool-type Reactor Cover: A 12° Sector

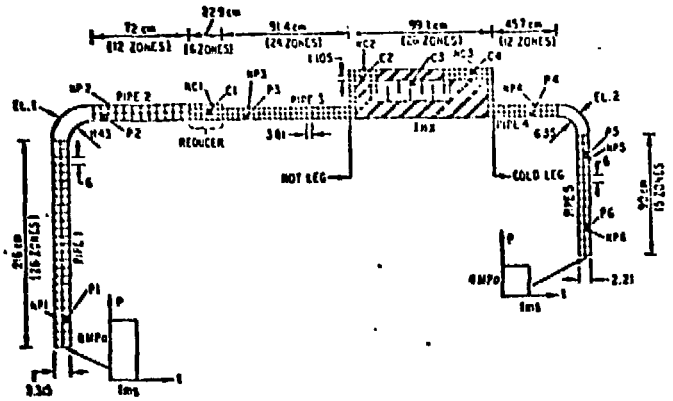

Fig. 3. Mathematical Model of the 1/10 Scale IHX within a Simplified Heat Transport System

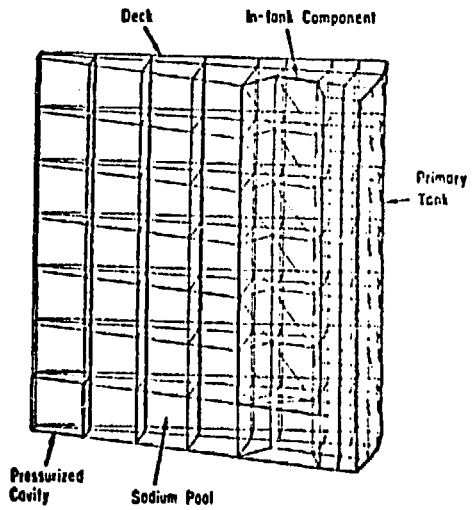

Fig. 4. A 12° Sector of a Primary Tank with Finite Element Mesh of the Fluid and the In-Tank Component

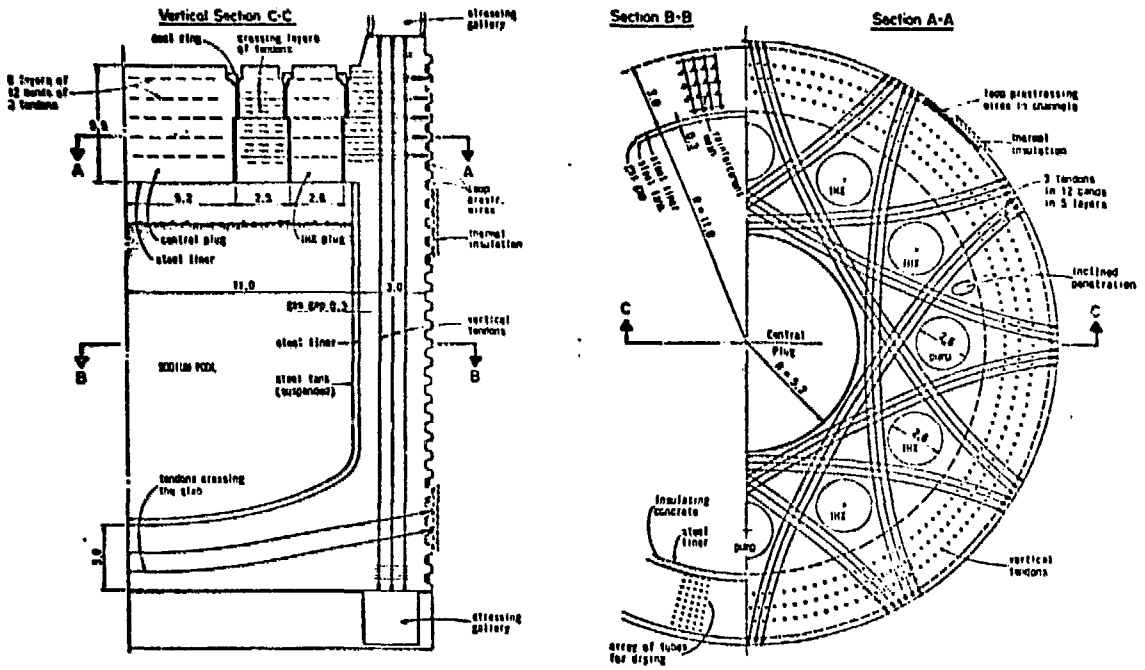

Fig. 5. A conceptual Design of PCRV for a Pool-type LMFBR

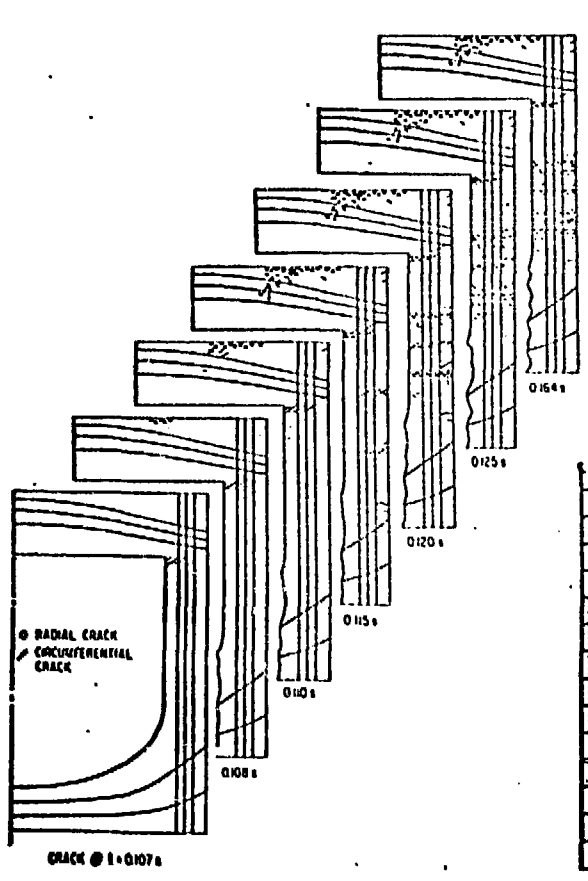

Fig. 6. Cracking Sequence of Pool-type PCRV during an HCDA

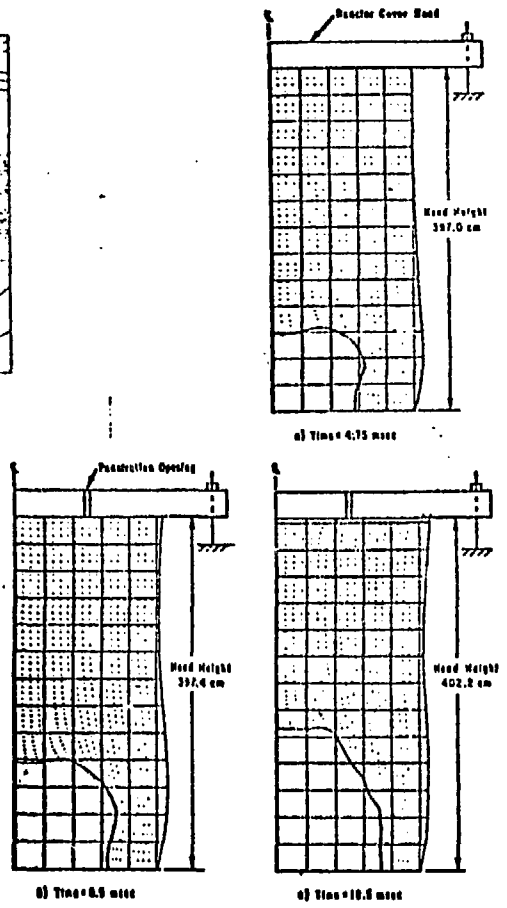

Fig. 7. ICECO Treatment of Sodium Spillage

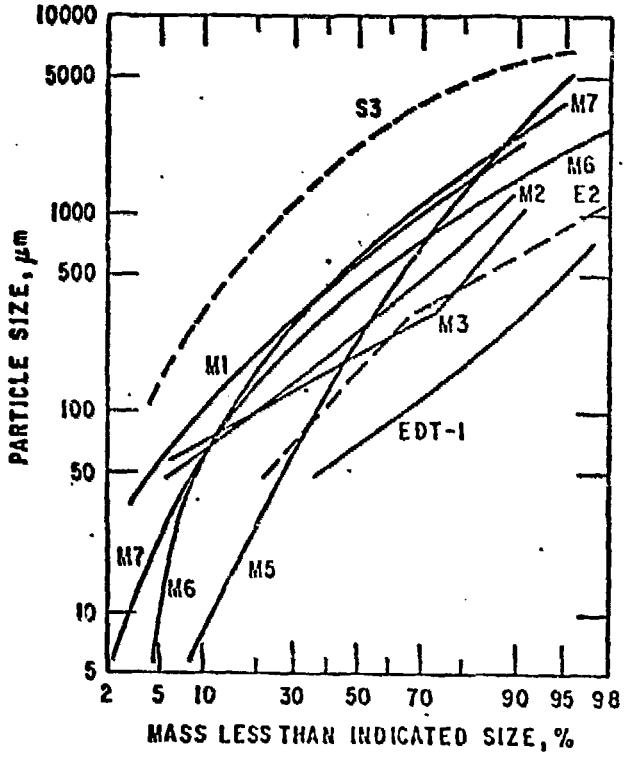

Fig. 8. Particle Size Distributions from Molten Fuel-Sodium Interaction Experiments

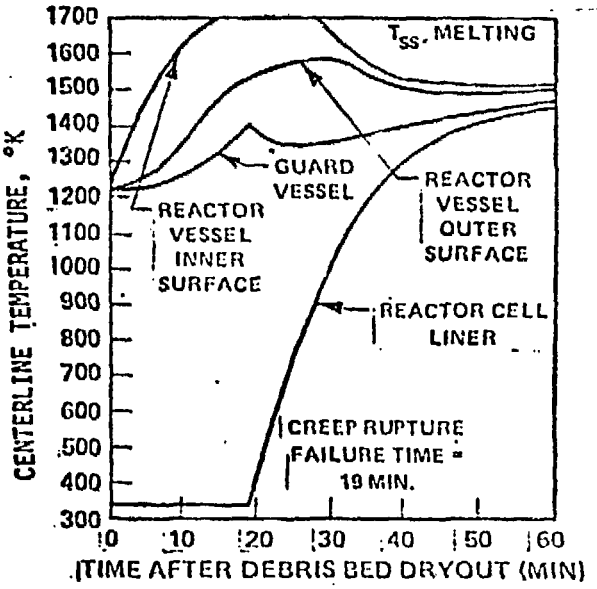

Fig. 9. Post-Dryout Thermal Response of Reactor Vessel, Guard Vessel, and Cell Liner

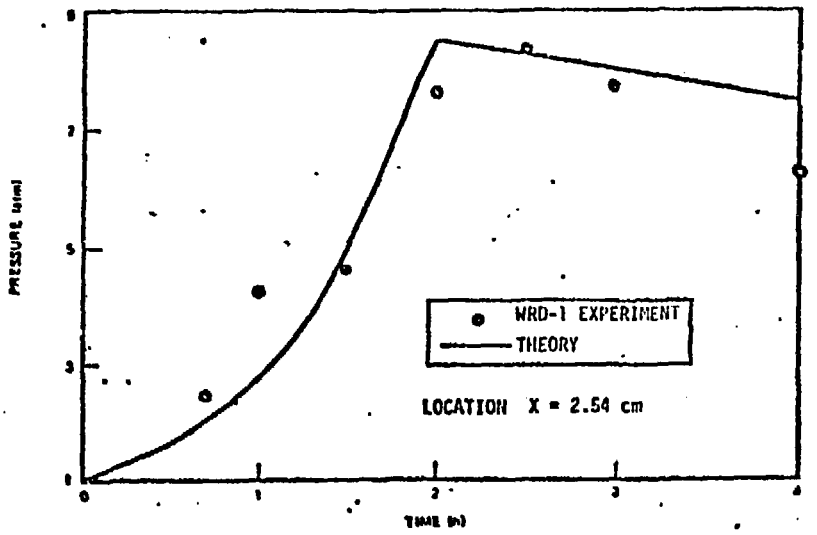

Fig. 10. Pressure Response in a Surface-Heated Magnetite Concrete Slab

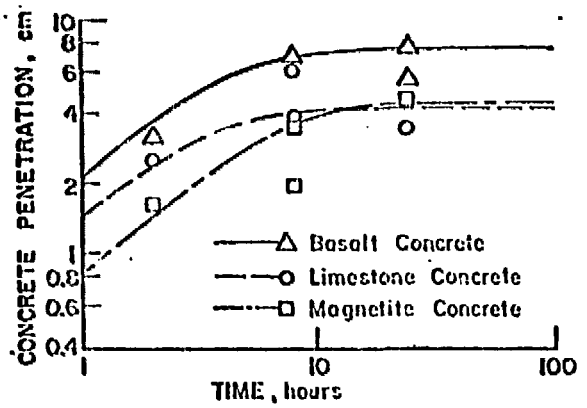

Fig. 11. Sodium Penetration of Concrete at 677 to 870°C

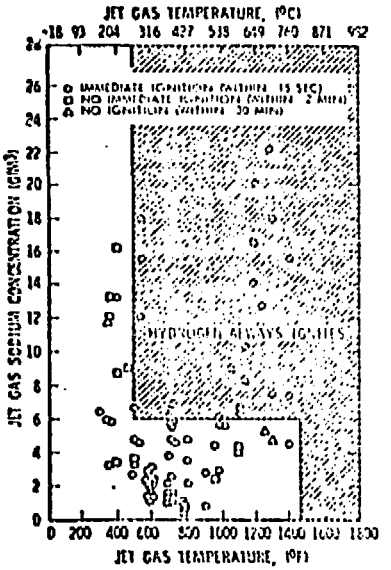

Fig. 12. Self-Ignition of a Hydrogen and Sodium Vapor-Aerosol Jet into Air

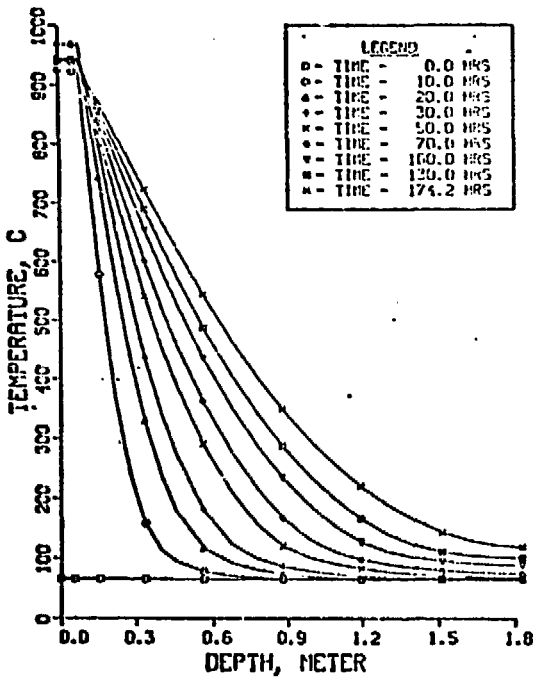

Fig. 13. CACECO Analysis, Structural Temperatures of Cavity Floor Concrete

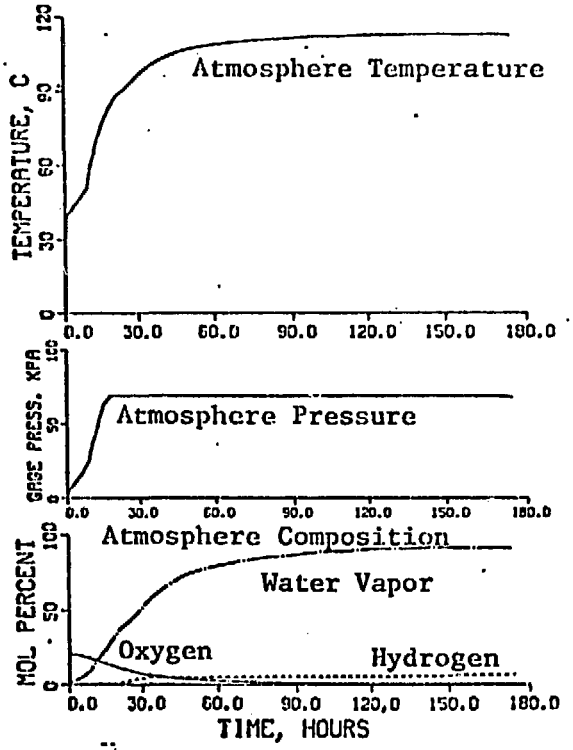

Fig. 14. CACECO Analysis, Building Atmosphere Conditions